



Cite this: RSC Adv., 2017, 7, 6000

## Silicone oil promotes amyloid-like aggregation of $\alpha$ B-crystallin

Zhiwei Shen,<sup>ab</sup> Qiqige Du,<sup>a</sup> Haozhi Lei,<sup>ab</sup> Yuhui Wei,<sup>a</sup> Jun Hu<sup>\*a</sup> and Yi Zhang<sup>\*a</sup>

Silicone oil is a chemically inert and biocompatible material. However, the use of silicone oil as an adjunct for internal tamponade in the treatment of retinal detachment is accompanied by the sequelae of cataract, the molecular mechanism of which has been a mystery for scientists. In this study, we focused on the influence of silicone oil on the aggregating behaviors of one of the important proteins in the eyes,  $\alpha$ B-crystallin (CRYAB). We found that silicone oil could promote the amyloid-like aggregation of CRYAB, verified using atomic force microscopy (AFM), transmission electron microscopy (TEM), laser granularity and number analysis (Nanosight), and turbidity measurements. Furthermore, fluorescent experiments using Thioflavin T (ThT), Congo red, and 1-anilinonaphthalene-8-sulfonic acid (ANS) suggested formation of a  $\beta$ -sheet structure in CRYAB in the presence of silicone oil, which was also confirmed by far-UV circular dichroism (CD) spectroscopy. These findings provide a direct evidence of the changes in the secondary structures of CRYAB protein and amyloid aggregation behavior upon adding silicone oil in the solution, and could be helpful for understanding the molecular mechanisms of the cataract formed in silicone oil-filled eyes.

Received 22nd November 2016  
Accepted 7th January 2017

DOI: 10.1039/c6ra27128f

[www.rsc.org/advances](http://www.rsc.org/advances)

## Introduction

Silicone oil has been widely used in medical care, particularly as an internal tamponade material in the treatment of complicated retinal detachment, owing to its outstanding properties: low biotoxicity, chemical inertness, suitable density, and surface tension.<sup>1</sup> It has been shown to be especially beneficial in eyes with proliferative vitreoretinopathy after pars plana vitrectomy (PPV) with intraocular gas tamponade,<sup>2</sup> in traumatic hemophthalmos with secondary retinal detachment, and in eyes with advanced proliferative diabetic retinopathy with widespread tractional retinal detachment.<sup>3</sup> However, the use of silicone oil is accompanied by a series of complications: keratopathy,<sup>4</sup> anterior chamber oil emulsification,<sup>5,6</sup> glaucoma, and cataract.<sup>7-15</sup> Posterior subcapsular cataract has been found in many cases in silicone oil-filled eyes.<sup>7,16</sup>

Silicone oil is a chemically inert material, and the complications it causes in the eyes are a mystery for scientists. Over the past decades, many efforts have been made to investigate the mechanism of silicone oil-induced cataract, which may involve the following factors: (1) bright and long-time illumination, leading to changes in the transparency of the lens;<sup>17,18</sup> (2) increase in oxygen tension in the glass body, which increases the risk of occurrence of nuclear cataract;<sup>19,20</sup> (3) changes in the

metabolism of lens;<sup>21</sup> (4) causation of an inflammatory reaction.<sup>22</sup> The exact mechanism remains unknown because of the lack of the research at the molecular level. For example, there is no report on the influence of silicone oil on the key biomolecules in cataract.

Crystallin proteins are important proteins in the eyes that form amyloid fibril,<sup>23</sup> and their aggregation is the most important factor in cataract formation.<sup>24</sup> Crystallins are divided into  $\alpha$ ,  $\beta$ , and  $\gamma$  families, but the functions of  $\beta$ - and  $\gamma$ -crystallin proteins in mammalian lenses are not yet clear. The  $\alpha$ -crystallins, which are further divided into  $\alpha$ A- and  $\alpha$ B-crystallins, can reach concentration levels of about 50% of the total structural protein mass of the lens.<sup>25</sup> They function as structural proteins, as well as molecular chaperones, to prevent aggregation and precipitation of  $\beta$  and  $\gamma$ -crystallins and to delay lens opacification.<sup>26</sup> The  $\alpha$ -crystallins, especially  $\alpha$ B-crystallin (CRYAB), are also extensively distributed outside the lens.<sup>27-29</sup> The CRYAB protein is over-expressed in many neurological diseases, and mutations in  $\alpha$ A or  $\alpha$ B-crystallin can cause cataract and myopathy.<sup>30</sup> It will be interesting to see if silicone oil would influence the aggregation of crystallins.

Silicone oil has been reported to induce unordered amorphous aggregation of proteins.<sup>31,32</sup> We speculate that cataract may also be related to the possible aggregation of crystallin proteins in silicone oil-filled eyes, where high concentrations and highly-ordered structures of crystallin proteins in the lens contribute to its transparency.<sup>30</sup> In this study, silicone oil was added to an aqueous solution of CRYAB, and the aggregation of CRYAB was characterized using a variety of methods. It was

<sup>a</sup>Key Laboratory of Interfacial Physics and Technology, Shanghai Institute of Applied Physics, Chinese Academy of Sciences, Shanghai 201800, China. E-mail: zhangyi@sinap.ac.cn; hujun@sinap.ac.cn

<sup>b</sup>University of Chinese Academy of Sciences, Beijing 100049, China



found that silicone oil could indeed accelerate the aggregation of CRYAB. Structural studies showed formation of more  $\beta$ -sheets in the proteins upon addition of silicon oil, which led to the formation of amyloid-like protein nanostructures. These experimental results should be helpful for understanding the molecular mechanisms of silicone oil-induced cataract formation.

## Materials and methods

### Materials

Recombinant human crystallin alpha B (CRYAB) (HSP-003) was purchased from ProSpec (ISR). CRYAB produced from *Escherichia coli* is a single, non-glycosylated polypeptide chain containing 175 amino acids with a molecular mass of 20.1 kDa. CRYAB was purified using proprietary chromatographic techniques at a concentration of 1 mg mL<sup>-1</sup>. Medical fluid silicone oil (350CST) was purchased from Dow Corning (USA). 1-Anilinonaphthalene-8-sulfonic acid (ANS), Congo red, Thioflavin T (ThT) were purchased from Sigma (USA). All other chemicals were of reagent grade and purchased from Sigma (USA), unless otherwise specified.

### Preparation of stock solutions

CRYAB was dissolved in buffer A (20 mM Tris-HCl, 50 mM NaCl, 1 mM EDTA, pH 7.5). A stock solution (suspension) of 1% (w/v) silicone oil was prepared by mixing silicone oil and buffer A in a 1.5 mL polypropylene centrifuge tube, followed by sonication for 45 min, and centrifugation at 5000 rpm for 5 min. The precipitate in the silicone oil suspension was discarded. Silicone oil suspensions were freshly prepared on the day they were used.<sup>32</sup> To avoid the influence of the lubricant silicone oil on the wall of plastic products,<sup>31</sup> all centrifuge tubes and pipette tips were ultrasonicated alternately in anhydrous ethanol and water thrice for an hour each.

### Turbidity measurement

Turbidity measurements of the mixture of CRYAB (1 mg mL<sup>-1</sup>) and silicone oil in buffer A (v/v = 1 : 1) were performed by monitoring the absorbance at 280 nm, using a U-3010 spectrophotometer (HITACHI, Japan). Three measurements were performed, and the readings were averaged after subtracting the buffer baseline.

### CRYAB aggregation of granularity and number analysis

The 1 : 1 (v/v) mixture of CRYAB (final concentration 0.5 mg mL<sup>-1</sup>) and silicone oil (final concentration 0.5%) in buffer A was incubated at 60 °C for certain time. Then, the mixture was diluted 100 times and tested with Nanosight NS300 (Malvern, UK) for granularity and number analysis. NTA 3.2 software was used for capturing and analyzing the data.<sup>33</sup> Data from each group were averaged from five tests. The NTA software was then able to identify and track individual nanoparticles moving under Brownian motion and relate the movement to a particle size, according to the following formula derived from the Stokes-Einstein equation:

$$\overline{(x, y)^2} = \frac{2k_B T}{3r_h \pi \eta}$$

where  $k_B$  is the Boltzmann constant,  $\overline{(x, y)^2}$  the mean squared speed of a particle at a temperature  $T$  in a medium of viscosity  $\eta$  with a hydrodynamic radius of  $r_h$ .<sup>33</sup>

### 1-Anilinonaphthalene-8-sulfonic acid (ANS) fluorescence spectroscopy

The mixture of CRYAB sample solutions (final concentration 0.1 mg mL<sup>-1</sup>), ANS (final concentration 20 mM), and silicone oil (final concentration 0.05%) in buffer A was incubated in dark for a few minutes at room temperature. ANS fluorescence emission intensity at 470 nm was recorded by exciting samples at 380 nm using a spectrophotometer (Edinburgh Instruments FS920, UK).

### Thioflavin T (ThT) fluorescence measurement

ThT was dissolved in buffer A, and then mixed with CRYAB (final concentration 0.1 mg mL<sup>-1</sup>) and silicone oil (final concentration 0.05%) to a final concentration of 20  $\mu$ M. The ThT fluorescence emission intensity at 480 nm was recorded at an excitation wavelength of 440 nm using a spectrophotometer (Edinburgh Instruments FS920, UK).

### Atomic force microscopy (AFM) and transmission electron microscopy (TEM) observations

The mixture of CRYAB (final concentration 0.5 mg mL<sup>-1</sup>) and silicone oil (final concentration 0.5%) in buffer A was incubated at 60 °C for a certain time. To prepare sample for AFM imaging, the mixture was diluted 100 times with buffer A, containing silicone oil (final concentration 0.5%). A drop of 30  $\mu$ L of the diluted solution was placed on a (3-aminopropyl) triethoxysilane-modified mica substrate.<sup>34</sup> The sample solution was allowed to adsorb for 3 min, then washed gently with water, followed by air drying. A commercial AFM (Multimode Nanoscope V, Veeco, Santa Barbara, CA) equipped with a J scanner was employed to reveal the CRYAB aggregate morphology. Experiments were performed in tapping mode. Silicon cantilevers with a nominal spring constant of 48 N m<sup>-1</sup> (NSC11, MikroMasch) were used. All AFM operations were carried out in air at room temperature.

CRYAB sample (5  $\mu$ L) was applied to glow-discharged carbon films on 400 mesh copper grids and stained with 2.5% uranyl formate for 30 s. Specimens were examined using Tecnai G2 TEM operated at an accelerating voltage of 120 kV. Images were recorded using a 4k  $\times$  4k charge-coupled device camera (BM-Eagle, FEI Tecnai).

### Congo red staining

The mixture of CRYAB (final concentration 0.5 mg mL<sup>-1</sup>) and 0.5% silicone oil was incubated at 60 °C for 2 h. Then the mixture was centrifuged at 15 000  $\times$  g for 20 min. The sediment was resuspended using 100  $\mu$ L buffer A containing 0.1 mg mL<sup>-1</sup> Congo red and incubated for 10 min at room temperature. The mixture was centrifuged again at 15 000  $\times$  g for 20 min. The



supernatant containing Congo red was discarded, while the sediment was resuspended in 30  $\mu$ L water. The washing procedure was repeated several times until the supernatant was no longer red. The sediment was finally resuspended with 5  $\mu$ L water and pipetted onto a glass coverslip. After drying at room temperature, samples were observed using an optical microscope equipped with cross-polarizers.<sup>35</sup>

### Far-UV CD spectroscopy

The change in the secondary structure of CRYAB in the presence of silicone oil was evaluated using far-UV CD spectroscopy. CD spectra of the mixture of CRYAB (final concentration 0.2 mg mL<sup>-1</sup>) and silicone oil (final concentration 0.5%) in buffer A were recorded over the wavelength range of 195–260 nm using a Chirascan (Applied Photophysics, UK) with a 0.1 cm path length sample cell. Buffer A was used as control. All CD measurements were performed at room temperature using a bandwidth of 1.0 nm, a step interval of 1 nm, and a scanning speed of 50 nm min<sup>-1</sup>. Each CD spectrum was averaged from three scans, and the corresponding baseline of buffer was subtracted from the sample spectrum. The secondary structures of CRYAB samples were analyzed using CDNN program.

## Results and discussion

### Effect of silicone oil on aggregation of CRYAB

The extent of aggregation of CRYAB in the presence of silicone oil was evaluated by measuring the turbidity of CRYAB samples at 280 nm after incubation for 1 or 2 days at room temperature. As shown in Fig. 1a, though CRYAB itself aggregated to some extent with an increased turbidity after incubation for 24 h and 48 h, adding silicone oil into the CRYAB solution resulted in a sharp increase in the turbidity, indicating an accelerated aggregation process. In addition, we measured UV absorbance of the samples that were incubated for 4 weeks at 37 °C. As shown in Fig. 1b, the absorbance (and thus the turbidity) of CRYAB solution containing silicone oil was notably higher than that of the pure CRYAB solution even after incubation for such a long time. This result indicates that silicone oil promotes CRYAB aggregation in a long-acting way.

The size and quantity of the aggregated CRYAB were studied using a laser particle size analyzer, Nanosight. The resolution of Nanosight is between 30 nm and 1000 nm.<sup>33</sup> Therefore, we

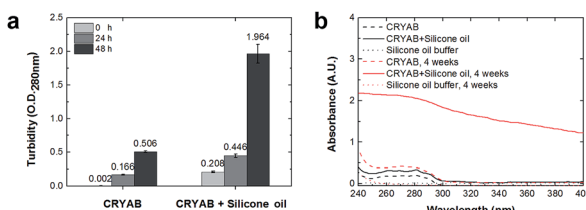


Fig. 1 (a) Turbidity measurements of CRYAB in the presence of silicone oil. Each data was averaged from 3 independent experiments. (b) Absorbance of CRYAB solutions with or without silicone oil after incubation for 4 weeks at 37 °C.

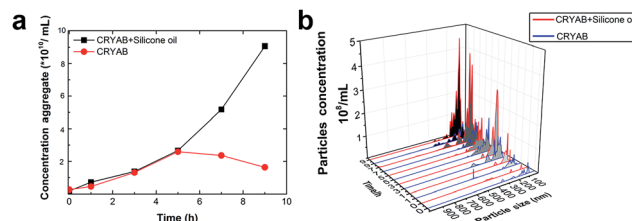


Fig. 2 Effect of silicone oil on the size and quantity of protein aggregates. (a) Evolution of CRYAB aggregate concentration during incubation. (b) Size distribution of CRYAB aggregates.

produced large protein aggregates by accelerating the reversible protein aggregation process at an elevated temperature of 60 °C.<sup>36</sup> Fig. 2a illustrates the evolution of the CRYAB particle concentration (number of total aggregated CRYAB particles in a unit volume) during incubation. In the first five hours, the CRYAB aggregate concentration increased in a similar manner in all solutions, irrespective of the presence of silicone oil. After that, the CRYAB aggregate concentration in the pure protein solution started to decrease, probably due to the fusion of small aggregates to form large ones. In contrast, the CRYAB aggregate concentration in the protein solution with silicone oil increased during the entire experimental period, indicating continuous formation of new protein aggregates. It is worth noting that the concentration of silicone oil particles in buffer was at least two orders of magnitude lower than those in the samples, and was thereby negligible for our study. Fig. 2b shows the evolution of the size distribution of CRYAB aggregates during incubation, which clearly indicates that most CRYAB aggregates had a size less than 300 nm. Particularly, there were more CRYAB aggregates with a size less than 200 nm formed after incubation with silicone oil for 5 h or more than those in the pure CRYAB solution. It is, thus, obvious that silicone oil accelerated the CRYAB aggregation to form CRYAB aggregates had a size less than 300 nm. Particularly, there were more CRYAB aggregates with a size less than 200 nm formed after incubation with silicone oil for 5 h or more than those in the pure CRYAB solution. It is, thus, obvious that silicone oil accelerated the CRYAB aggregation to form many large protein aggregates, which is consistent with the previously reported aggregation of proteins induced by silicone oil.<sup>32,37,38</sup>

### Amyloid-like aggregation of CRYAB in the presence of silicone oil

In order to know whether the CRYAB protein changed its structure in the presence of silicone oil, 1-anilinonaphthalene-8-sulfonic acid (ANS), fluorescent spectra were recorded. ANS is a hydrophobic fluorescent dye, which is usually used to stain globular proteins upon exposure of the hydrophobic core of proteins in solvents.<sup>39</sup> Crystallin proteins are known to be highly hydrophilic, and are present in high concentrations in the crystalline lens to maintain lens transparency.<sup>38</sup> However, we observed a sharp increase in the ANS fluorescent intensity of the CRYAB solution containing silicone oil (Fig. 3a). This result indicates that the presence of silicone oil led to the exposure of



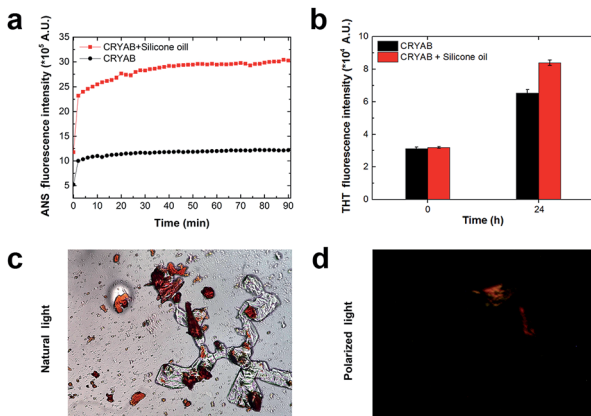


Fig. 3 Fluorescent studies indicating the change in molecular conformation of CRYAB in the presence of silicone oil. (a) Dynamic scanning of ANS fluorescence intensity. Data was collected every two minutes. The fluorescence intensity of the silicone oil in buffer was about  $1 \times 10^5$ , which could be neglected, since this value is much lower than that of the protein solutions. (b) ThT fluorescence intensity of CRYAB. Each data was averaged from 3 independent experiments. (c) Representative natural light microscopy image of Congo red-stained CRYAB aggregates. (d) Image of Congo red-stained CRYAB aggregates under cross polarized light.

the hydrophobic core of CRYAB in solution. The ANS fluorescent intensity increased immediately after mixing of the protein and the silicone oil, suggesting that the protein exposed its hydrophobic core quickly. We hypothesize that the hydrophobic silicone oil molecule may maintain the structure of the core-exposed CRYAB protein and act as a seed for its nucleation.<sup>40–42</sup> Then CRYAB monomers could add to the seeds to form long fibrils, following the classic nucleation-growth mechanism.<sup>43–46</sup>

To understand if the aggregated species were unordered amorphous aggregates or ordered amyloid fibrils, we monitored the changes in Thioflavin T (ThT) and Congo red fluorescent emissions in solutions with or without silicone oil. ThT has been used as a molecular probe to detect the  $\beta$ -sheet structure in proteins during the formation of amyloid aggregates.<sup>47</sup> It was found that the intensity of ThT fluorescence increased after incubation with CRYAB. However, it increased to a higher level in CRYAB with silicone oil than in the pure protein solution (Fig. 3b). This difference was observed in all ThT experiments. Similarly, Congo red staining is also widely used to determine the existence of  $\beta$ -sheet structure in proteins.<sup>48,49</sup> In our experiments, Congo red-stained CRYAB aggregates formed in the presence of silicone oil appeared red under a normal optical microscope (Fig. 3c) and yellow-green under cross-polarized light (Fig. 3d), indicating the existence of  $\beta$ -sheet in CRYAB. These fluorescent studies suggest that CRYAB protein easily formed amyloid-like aggregation *in vitro*, which is consistent with previous reports,<sup>50</sup> and silicone oil promoted the formation of a  $\beta$ -sheet secondary structure such that it accelerated the protein aggregation process.

To further understand the role of silicone oil in the changes in secondary structure of CRYAB, far-UV circular dichroism (CD) spectra were monitored (Fig. 4a). Among these spectra, the

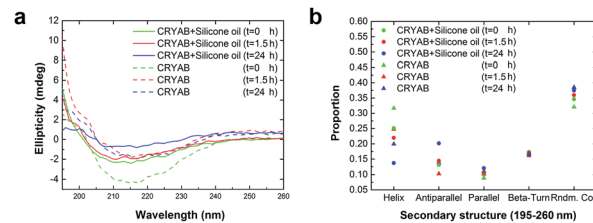


Fig. 4 Far-UV CD study of the CRYAB. (a) Spectra of CRYAB solution incubated with (solid lines) or without (dotted lines) silicone oil. (b) Software analysis of the far-UV CD spectra in the range of 195–260 nm revealing the ratio of each kind of secondary structure of CRYAB.

spectrum of CRYAB incubated with silicone oil for the longest time (solid blue line) showed the most drastic difference from its original protein state (dotted green line), indicating a sharp change in secondary structures. Based on these spectra, secondary structure calculations were done using CDNN program, which provided quantitative information about the secondary structures of CRYAB: percentages of  $\alpha$ -helix,  $\beta$ -antiparallel and  $\beta$ -parallel,  $\beta$ -turn, and random coils (Fig. 4b). In both types of CRYAB solutions, those incubated with and without silicone oil, an increase in the percentages of  $\beta$ -antiparallel and random coils, and a decrease in those of  $\alpha$ -helices were observed. In particular, a 20% increase in the content of  $\beta$ -antiparallel sheets was observed in CRYAB solution incubated with silicone oil for 24 h, in contrast to only 13% increase in pure CRYAB solution (Fig. 4b), suggesting that silicone oil promoted the formation of a  $\beta$ -antiparallel structure. The secondary structures,  $\beta$ -parallel and  $\beta$ -turn, changed relatively little, implying a spherical to linear transformation of the protein structure. Obviously, CRYAB is quite different from other proteins that were previously reported, which showed no changes in their secondary structures.<sup>31,32</sup>

### Aggregate morphology of CRYAB

Finally, the morphology of the CRYAB amyloid aggregates was investigated using atomic force microscopy (AFM). In general, CRYAB monomers assembled into short fibrils in the first several hours, which further formed large aggregates (Fig. 5a and b). The fibrils had a height of 9–10 nm and an apparent width of about 40 nm. Considering the tip convolution effect,<sup>51,52</sup> the deconvoluted width of the fibrils would be  $\sim 20$  nm in case an AFM tip with a radius of 10 nm was used in the experiment. Furthermore, the morphology of CRYAB fibrils obtained after 2 h incubation was studied using TEM (Fig. 5c and d). Statistical analyses from the TEM images indicated widths of  $15.7 \pm 1.2$  nm ( $N = 50$ ) and  $16.5 \pm 1.5$  nm ( $N = 50$ ), respectively, for CRYAB fibrils obtained after incubation with or without silicone oil. The morphologies of the short fibrils were similar to those previously reported.<sup>23</sup> The formation of short fibrils and large aggregates also indicates a heterogeneous multimeric assembly of the protein.<sup>30</sup>

From the AFM and TEM experiments, no obvious difference was found in the morphology of the short fibrils and aggregates that were formed by CRYAB with or without silicone oil,



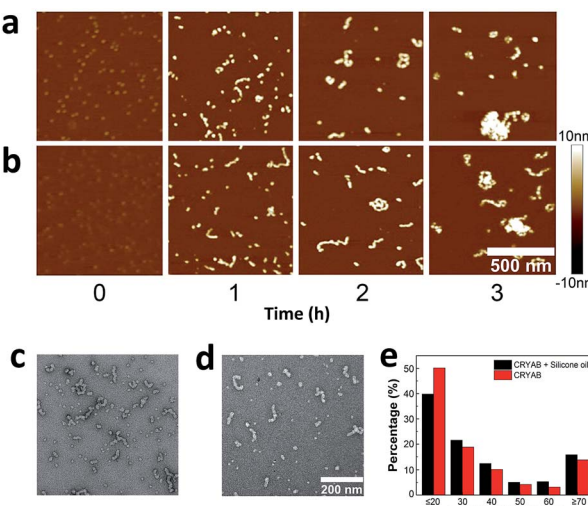


Fig. 5 (a-d) Typical AFM (a and b) and TEM (c and d) images of CRYAB aggregates. (a and d) Pure CRYAB solution. (b and c) CRYAB solution incubated with silicone oil. Numbers 0 to 3 indicate the incubation time. The incubation time of samples for TEM measurement was 2 h. The lateral and Z scale bars shown in (b) apply to all AFM images. The lateral scale bar shown in (d) also applies to (c). (e) The distribution of contour lengths of fibrils statistically measured from TEM images. For short fibrils or round-shaped particles, their longest contour lengths were measured. In total 287 and 417 fibrils were measured from pure CRYAB and CRYAB with silicone oil, respectively.

suggesting that silicone oil may not change the structure of the protein aggregates. However, large aggregates were more frequently observed in the late incubation solution of CRYAB with silicone oil. For example, as shown in Fig. 5e, pure CRYAB samples contained higher ratio of shorter particles less than 20 nm (probably oligomers), while the CRYAB samples incubated with silicone oil contained higher ratio of longer fibrils.

Previous studies showed that silicone oil only induced an amorphous aggregation of proteins, with no change in the secondary structure of the proteins.<sup>31,32</sup> However, our results clearly indicated that silicone oil induced a change in secondary structure in CRYAB, and promoted amyloid-like aggregation of the protein, as verified using AFM and TEM morphology study, ThT fluorescence and Congo red staining analyses, and far-UV CD spectroscopy. It seems that silicone oil has direct effects on the intramolecular interactions responsible for conformation transformation, probably through interaction with the hydrophobic core of CRYAB protein.

## Conclusion

In summary, we studied the effect of silicone oil on the aggregation of CRYAB using a variety of methods. Measurements of the turbidity of CRYAB solution and aggregate size and concentration of the protein confirmed that silicone oil was able to promote the formation of numerous and large CRYAB aggregates. ThT, Congo red, and ANS fluorescent analyses of the protein aggregates suggested the formation of  $\beta$ -sheet structure in the CRYAB in the presence of silicone oil, which further

assembled into nanometer-sized amyloid aggregates. The change in the secondary structure of CRYAB in the presence of silicone oil was also confirmed by CD spectroscopy. AFM studies revealed that CRYAB assembled into short fibrils and large aggregates. These findings provide direct evidence of the changes in secondary structures of CRYAB protein and amyloid-like aggregation upon adding silicone oil in the solution, and should be helpful for understanding the molecular mechanisms of cataract formed in silicone oil-filled eyes. In addition, as silicone oil is able to migrate to the brain,<sup>53,54</sup> our results call for a test study of the possible risk of the silicone oil-induced amyloid aggregation in neurodegenerative disease-related proteins in the brain, which could be the focus of our future research.

## Acknowledgements

This work was financially supported by the National Basic Research Program of China (No. 2013CB932801), the National Natural Science Foundation of China (No. 11274334 and 11674344), and the Chinese Academy of Sciences (grant No. KJZD-EW-M03).

## Notes and references

- 1 P. Ichhpujani, A. Jindal and L. J. Katz, *Graefe's Arch. Clin. Exp. Ophthalmol.*, 2009, **247**, 1585–1593.
- 2 G. W. Abrams, S. P. Azen, M. C. B. Nd, H. W. Flynn, M. Y. Lai and S. J. Ryan, *Am. J. Ophthalmol.*, 1997, **115**, 335–344.
- 3 M. Gonvers, *Am. J. Ophthalmol.*, 1985, **100**, 239–245.
- 4 K. G. Riedel, V. P. Gabel, L. Neubauer, A. Kampik and O. E. Lund, *Graefe's Arch. Clin. Exp. Ophthalmol.*, 1990, **228**, 19–23.
- 5 J. L. Federman and H. D. Schubert, *Ophthalmology*, 1988, **95**, 870–876.
- 6 A. Crisp, E. Dejuan and J. Tiedeman, *Arch. Ophthalmol.*, 1987, **105**, 546–550.
- 7 D. Borislav, *Doc. Ophthalmol.*, 1993, **83**, 79–82.
- 8 C. C. Barr, M. Y. Lai, J. S. Lean, K. L. P. Linton, M. Trese, G. Abrams, S. J. Ryan and S. P. Azen, *Ophthalmology*, 1993, **100**, 1629–1635.
- 9 Q. H. Nguyen, M. A. Lloyd, D. K. Heuer, G. Baerveldt, D. S. Minckler, J. S. Lean and P. E. Liggett, *Ophthalmology*, 1992, **99**, 1520–1526.
- 10 E. Punnonen, L. Laatikainen, P. Ruusuvuara and K. Setälä, *Acta Ophthalmol.*, 1989, **67**, 30–36.
- 11 L. Zborowskigutman, G. Treister, N. Naveh, V. Chen and M. Blumenthal, *Br. J. Ophthalmol.*, 1987, **71**, 903–906.
- 12 A. G. Casswell and Z. J. Gregor, *Br. J. Ophthalmol.*, 1987, **71**, 898–902.
- 13 C. Chan and E. Okun, *Ophthalmology*, 1986, **93**, 651–660.
- 14 P. K. Leaver, R. H. Grey and A. Garner, *Br. J. Ophthalmol.*, 1979, **63**, 361–367.
- 15 P. A. Cibis, B. Becker, E. Okun and S. Canaan, *Arch. Ophthalmol.*, 1962, **68**, 590–599.
- 16 C. M. Gremillion, G. A. Peyman, K. R. Liu and K. S. Naguib, *Br. J. Ophthalmol.*, 1990, **74**, 643–646.

17 M. Dogramaci, K. Williams, E. Lee and T. H. Williamson, *Graefe's Arch. Clin. Exp. Ophthalmol.*, 2013, **251**, 35–39.

18 M. A. Mainster and P. L. Turner, *Am. J. Ophthalmol.*, 2010, **149**, 543–549.

19 B. M. Palmquist, B. Philipson and P. O. Barr, *Br. J. Ophthalmol.*, 1984, **68**, 113–117.

20 N. M. Holekamp, Y. B. Shui and D. C. Beebe, *Am. J. Ophthalmol.*, 2005, **139**, 302–310.

21 S. Saika, T. Miyamoto, T. Tanaka, Y. Ohnishi, A. Ooshima and W. Kimura, *J. Curr. Res. Sci.*, 2002, **28**, 376–378.

22 L. J. Wickham, R. H. Asaria, R. Alexander, P. Luthert and D. G. Charteris, *Br. J. Ophthalmol.*, 2007, **91**, 258–262.

23 H. Ecroyd and J. A. Carver, *Cell. Mol. Life Sci.*, 2008, **66**, 62–81.

24 K. L. Moreau and J. A. King, *Trends Mol. Med.*, 2012, **18**, 273–282.

25 H. Bloemendaal, J. W. De, R. Jaenicke, N. H. Lubsen, C. Slingsby and A. Tardieu, *Prog. Biophys. Mol. Biol.*, 2004, **86**, 407–485.

26 R. F. Fisher, *Molecular and Cellular Biology of the Eye Lens*, BMJ Group, 1982.

27 T. Iwaki, A. Kumeiaki and J. E. Goldman, *J. Histochem. Cytochem.*, 1990, **38**, 31–39.

28 R. A. Dubin, E. F. Wawrousek and J. Piatigorsky, *Mol. Cell. Biol.*, 1989, **9**, 1083–1091.

29 S. P. Bhat and C. N. Nagineni, *Biochem. Biophys. Res. Commun.*, 1989, **158**, 319–325.

30 J. Horwitz, *Exp. Eye Res.*, 2003, **76**, 145–153.

31 R. Thirumangalathu, S. Krishnan, M. S. Ricci, D. N. Brems, T. W. Randolph and J. F. Carpenter, *J. Pharm. Sci.*, 2009, **98**, 3167–3181.

32 L. S. Jones, A. Kaufmann and C. R. Middaugh, *J. Pharm. Sci.*, 2005, **94**, 918–927.

33 V. Filipe, A. Hawe and W. Jiskoot, *Pharm. Res.*, 2010, **27**, 796–810.

34 J. H. Lu, H. K. Li, H. J. An, G. H. Wang, Y. Wang, M. Q. Li, Y. Zhang and J. Hu, *J. Am. Chem. Soc.*, 2004, **126**, 11136–11137.

35 B. Dai, D. Li, W. Xi, F. Luo, X. Zhang, M. Zou, M. Cao, J. Hu, W. Y. Wang, G. H. Wei, Y. Zhang and C. Liu, *Proc. Natl. Acad. Sci. U. S. A.*, 2015, **112**, 2996–3001.

36 L. Zhao, X. J. Chen, J. Zhu, Y. B. Xi, X. Yang, L. D. Hu, H. Ouyang, S. H. Patel, X. Jin, D. Lin, F. Wu, K. Flagg, H. Cai, G. Li, G. Cao, Y. Lin, D. Chen, C. Wen, C. Chung, Y. Wang, A. Qiu, E. Yeh, W. Wang, X. Hu, S. Grob, R. Abagyan, Z. Su, H. C. Tjondro, X. J. Zhao, H. Luo, R. Hou, J. J. Perry, W. Gao, I. Kozak, D. Granet, Y. Li, X. Sun, J. Wang, L. Zhang, Y. Liu, Y. B. Yan and K. Zhang, *Nature*, 2015, **523**, 607–611.

37 R. Thirumangalathu and M. S. Krishnan Sricci, *J. Pharm. Sci.*, 2009, **98**, 3167–3181.

38 L. T. S. Jones, A. Kaufmann and C. R. Middaugh, *J. Pharm. Sci.*, 2005, **94**, 918–927.

39 I. Sirangelo, E. Bismuto, S. Tavassi and G. Irace, *Biochim. Biophys. Acta, Protein Struct. Mol. Enzymol.*, 1998, **1385**, 69–77.

40 M. Lankers and O. Valet, *PharmIndex*, 2012, **74**, 1533–1538.

41 R. D. Hills and B. C. Rd, *J. Mol. Biol.*, 2007, **368**, 894–901.

42 K. A. Dill, K. M. Fiebig and H. S. Chan, *Proc. Natl. Acad. Sci. U. S. A.*, 1993, **90**, 1942–1946.

43 J. S. Pedersen, G. Christensen and D. E. Otzen, *J. Mol. Biol.*, 2004, **341**, 575–588.

44 V. N. Uversky, J. Li, P. Souillac, I. S. Millett, S. Doniach, R. Jakes, M. Goedert and A. L. Fink, *J. Biol. Chem.*, 2002, **277**, 11970–11978.

45 T. R. Serio, A. G. Cashikar, A. S. Kowal, G. J. Sawicki, J. J. Moslehi, L. Serpell, M. F. Arnsdorf and S. L. Lindquist, *Science*, 2000, **289**, 1317–1321.

46 H. Naiki, N. Hashimoto, S. Suzuki, H. Kimura, K. Nakakuki and F. Gejyo, *Amyloid*, 1997, **4**, 223–232.

47 H. Levine, *Amyloid*, 1995, **2**, 1–6.

48 A. Lorenzo and B. A. Yankner, *Proc. Natl. Acad. Sci. U. S. A.*, 1995, **91**, 12243–12247.

49 K. Hsiao, P. Chapman, S. Nilsen, C. Eckman, Y. Harigaya, S. Younkin, F. Yang and G. Cole, *Science*, 1996, **274**, 99–102.

50 S. Meehan, Y. Berry, B. Luisi, C. M. Dobson, J. A. Carver and C. E. MacPhee, *J. Biol. Chem.*, 2004, **279**, 3413–3419.

51 S. Y. Fung, C. Keyes, J. Duhamel and P. Chen, *Biophys. J.*, 2003, **85**, 537–548.

52 C. L. Brown, I. A. Aksay, D. A. Saville and M. H. Hecht, *J. Am. Chem. Soc.*, 2002, **124**, 6846–6848.

53 S. Mathis, M. Boissonnot, J. P. Tasu, C. Simonet, J. Ciron and J. P. Neau, *Medicine*, 2016, **95**, e2359.

54 J. F. Kiilgaard, M. Dan, V. Løgager and M. L. Cour, *Acta Ophthalmol.*, 2011, **89**, 522–525.

